Proposed Model for Saturn's Auroral Response to the Solar Wind: Centrifugal Instability Model

E. C. Sittler, Jr.[1], M. F. Blanc[2] and J.D. Richardson[3]

1. NASA/Goddard Space Flight Center, MD, USA
2. Centre d'Etudes Spatiales des Rayonnements (CESR), Toulouse, France
3. Massachusetts Institute of Technology, MA, USA

We present a model of Saturn's global auroral response to the solar wind as observed by simultaneous Hubble Space Telescope (HST) auroral images and Cassini upstream measurements of the solar wind taken during the month of January 2004. These observations show a direct correlation between solar wind dynamic pressure and 1) auroral brightening toward dawn local time, 2) an increase of rotational movement of auroral features to as much as 75 % of the corotation speed, 3) the movement of the auroral oval to higher latitudes and 4) an increase in the intensity of Saturn Kilometric Radiation (SKR). Our model, referred to as the centrifugal instability model, provides an alternative to the reconnection model of *Cowley et al. [2004a,b]*; we suggest the above observations result from Saturn's magnetosphere being a fast rotator. Since the torques on Saturn's outer magnetosphere are relatively low, its outer magnetosphere will tend to conserve angular momentum. When compressed on the dayside, the outer magnetosphere spins up to higher angular velocities and when it expands, the outer magnetosphere spins down to lower angular velocities. This response occurs since Saturn's ionosphere is unable to enforce corotation. The outer boundary of the plasma sheet at L ~ 15 is

identified as the primary source location for the auroral precipitating particles. Enhanced wave activity, which can precipitate the auroral producing particles, may be present at this boundary. If radial transport is dominated by centrifugally driven flux tube interchange motions, when the magnetosphere spins up, outward transport will increase, and the precipitating particles will move radially outward (since the radial gradient in electron energy flux is negative). This mechanism will cause the auroral oval to move to higher latitudes as observed. The Kelvin-Helmholtz instability may contribute to the enhanced emission along the dawn meridian, as observed by HST, via enhanced wave activity and corresponding charged particle precipitation.

INTRODUCTION

Auroral structures and their dynamical response to the different momentum sources acting on a planetary magnetosphere are important tracers of magnetospheric dynamics and ionosphere/magnetosphere coupling. In this article, we propose a new qualitative model to explain the observed features of Saturn aurora's response to solar wind pressure changes. This model builds upon the relations between magnetospheric compression and expansion in response to solar wind pressure changes, plasma motions and overall rotation state, and auroral oval changes.

Magnetospheric compression and expansion properties

During the Voyager encounters, Saturn's magnetosphere was typically in a quiescent state [*Bridge et al,* 1981, 1982; *Ness et al.*, 1981, 1982; *Lazarus and McNutt,* 1983; *Sittler et al.*, 1983], with average magnetopause location at ~ 21 R_S near the nose of the magnetopause. At the time of Pioneer 11, the solar wind dynamic pressure was very high and the magnetosphere was compressed to a radial distance inside ~ 17.3 R_S [*Wolfe et al.*, 1980; *Smith et al.*, 1980a,b]. The observed movement of the magnetopause is consistent with a vacuum dipole, similar to that of the Earth but different from Jupiter (see Table 1 for list of compressibility indices and stand-off distances for Earth, Jupiter and Saturn).

Table 1

Parameter	Earth	Jupiter	Saturn
Compressibility Index	1/6	1/3	1/6.1
Stand-off Distance	8.8-11 R_E	47-67 R_J	17-21 R_S
Reference	5	4	1,2,3

1. Wolfe et al., Science, 207, 403, 1980. 2. Bridge et al., *Science*, **215**, 563, 1982. 3. Slavin et al., *Geophys. Res. Lett.*, **10(1)**, 9, 1983. 4. Bridge et al., *Science*, **204**, 987, 1979. 5. Holzer and Slavin, *J. Geophys. Res.*, **83(A8)**, 3831, 1978.

Magnetospheric plasma dynamics : rotation state and other motions

Pioneer 11 [*Frank et al.*, 1980] and Voyager [*Lazarus and McNutt*, 1983; *Richardson*, 1986] data showed that Saturn's magnetosphere is a fast rotator compared to Earth. For a

rotationally dominated magnetosphere, the convection electric field imposed by the solar wind is small relative to the rotational electric field of the planet's magnetosphere, $\left|\vec{E}_{conv} = -\eta\, \vec{V}_{SW} \times \vec{B}_{SW}\right| << \left|\vec{E}_{rot} = -\Omega R \times B_{Mag}\right|$ (with η ~ 5%, V_{SW} ~ 400 km/s, B_{SW} ~ 0.5 nT, ΩR ~ 60-120 km/s, B_{Mag} ~ 5 nT), a condition shown by *Sittler et al*. [2004] to be true for Saturn's magnetosphere under quiescent solar wind conditions. The parameter η gives the efficiency with which solar wind electric fields can penetrate into the magnetosphere. Here we note that *Cowley et al.* [2004a] prefer η ~ 15% when the magnetosphere is open, based on Earth observations by *Reiff et al.,* [1981]. For an efficiency of 5%, the stagnation point (located at 4 to 6 R_E near dusk at Earth) formed where the convection and corotation flows cancel, does not form at Saturn, since it would be located outside of the magnetospheric cavity. Thus at Saturn, plasma flows on closed flow lines encircling the planet throughout most of the magnetosphere, excluding the magnetotail and the immediate vicinity of magnetospheric boundaries. The rate of rotation of this plasma has been measured by Voyager 1 and 2 [*Richardson, 1986*] and more recently by Cassini within Saturn's inner plasmasphere [*Sittler et al., 2005*]. Figures 1 and 2, from *Richardson [1986],* shows the radial variation of the azimuthal and radial components of the flow. The flow is near corotation inside of r ~ 8 R_S. Using Cassini plasma data, *Sittler et al.* [*2005*], also show the azimuthal flow to be near corotation inside r ~ 8 R_S. Further out, *Richardon [1986]* shows that the plasma sub-corotates at larger radial distances. Figure shows a tendency for outward radial flows to anti-correlate with azimuthal flow velocities, consistent with outward drifting flux tubes conserving angular momentum, but there are exceptions, especially in the Voyager 1 data. To show this anti-correlation, we plot V_R versus V_ϕ in Figure 3.

Most of the Voyager 1 data have $V_R \sim 0$ over a wide range of normalized angular velocities $\Omega = V_\phi/V_{COR}$. If one excludes the clump of points with $V_R \sim +20$-40 km/s for $\Omega \sim 0.8$, there is a noticeable anti-correlation. The exluded points come from the outer magnetosphere toward noon, where the magnetosphere is compressed by the solar wind. This compression may simultaneously cause the flow to spin up at this local time and increase outward centrifugally driven transport. The anti-correlation between the Voyager 2 V_R and Ω values is convincing. Overall, the data are consistent with large scale, outward centrifugal transport with time dependent variations super-imposed.

Auroral response to solar wind pressure changes

The HST observations for the January 2004 campaign [*Clarke et al.*, 2005] and corresponding Cassini observations [*Crary et al.*, 2005], show: 1) that the auroral brightening correlates with solar wind dynamic pressure and is brightest on the dawn side; 2) that during a CIR passage the auroral features are moving at about 75% of corotation (auroral features move at 30-65 % of corotation at other times [*Clarke et al.*, 2005]); 3) that the auroral oval moves to higher magnetic latitudes when the magnetosphere is compressed and 4) that the auroral brightness correlates with Saturn Kilometric Radiation (SKR) intensity [*Kurth et al.*, 2005]. The partial corotation of auroral features suggests that they occur on flux tubes from the region of partial corotation in the external part of the Saturnian plasma sheet. As reported by *Gèrard et al.* [2004] and confirmed by *Clarke et al*. [2005], Saturn's aurora displays a spiraling pattern, moving in latitude as it rotates from dawn to noon to dusk and then back to dawn local

time. Earlier auroral observations had shown the aurora to be frequently brighter along the dawn meridian and fixed in local time (*Trauger et al.*, [1998]; *Cowley et al*., [2003] and *Gèrard et al.,* [2004]). The auroral brightening on the dawn side reported by *Clarke et al. [2005],* displayed a patchiness which may provide an important constraint for any proposed model. A typical value for the angular velocity of the rotating plasma in the outer magnetosphere, Ω, is ~ 50% of corotation Ω_{cor} [*Lazarus and McNutt, 1983; Richardson, 1986; Cowley and Bunce, 2003*], based on the very limited snapshots provided by the two Voyager fly-bys. We compare these characteristics with those observed at Earth and Jupiter. Although the aurora at Earth can be quite complex, since it spreads both poleward and equatorward during a magnetic storm, the general tendency is for the aurora to move equatorward as the ring current intensifies [*Elphinstone et al.*, 1996]. This response is contrary to that observed in Saturn.

Table 2

Type	LT Properties	Characteristic	Reference
Outer O	$\|\lambda\|<70°$ Partial oval centered on midnight	Faint & Diffuse	1
Quiet-Expanded QE	$\lambda \sim -72°$ LT 06, $\lambda \sim -74°$ LT 12 & $\lambda \sim -72°$ LT 18	Rotating arc ~ 70% CR LT 06, 55% CR LT 12 & 20% CR LT 18	1
Quiet-Moderate QM	$\lambda \sim -77°$ LT00, $\lambda \sim -73°$ LT 06, $\lambda \sim -75°$ LT 12, $\lambda \sim -72.5°$ LT 18	Tighter rotating arc with spiral shape. Rotation same as QE	1
Shock 1 S1	$-80° < \lambda < -75°$	Tight rotating arc, medium intensity toward dawn	1
Shock 2 S2	$-82° < \lambda < -76°$	Very tight rotating arc with high intensity to dawn	1
Relaxation R	$\lambda \sim -72°$ LT 06, $\lambda \sim -75°$ LT 07-09, $\lambda \sim -78°$ LT 18	Occurs after S2 with tight rotating arc moving to smaller λ,	1

		brighter toward dawn.	
Upstream Unknown Dec. 8, 2000	$\lambda \sim 72°$ at dawn, 75° pre-noon & ~ 78° in afternoon	Moderate intensity with max pre-noon.	2
Cassini upstream	$\lambda \sim 72°$ to > 82° at dawn, very intense, rotation increases.	Movement of spiral to higher λ during CIR	3
Upstream Unknown 10/1997-01/2001	Oval 70° to 80°, dawn intense, dusk weak & diffuse.	Discover spiral structure of aurora	4

1. Grodent et al. [2005], 2. Cowley et al. [2004a], 3. Clarke et al. [2005], 4. Gèrard et al. [2004]. Note: Low ~ 1 kR, Medium ~ 50 kR & High ~ 120 kR intensity.

A more comprehensive description of the January 2004 campaign is given by Grodent et al. [2005]. Their results plus those of the other investigators discussed above are summarized in Table 2. Several morphological characteristics of Saturn's aurora were identified during the January 2004 campaign: 1.) An outer (O) region with weak and diffuse emissions at low latitudes $\lambda < 70°$, 2.) A quiet-expanded (QE) feature which occurred during a rarefraction region in the solar wind and had a spiral structure with $\Omega \sim$ 65% near dawn, ~ 55% post-noon and ~ 20% at dusk, 3.) A quiet-moderate (QM) feature, which occurred when the upstream conditions were moderately intense, similar to QE but brighter with tighter oval toward higher latitudes as described above, 4.) A shock related feature (S1) due to passage of a moderate shock with ram pressure pulse of ~ 0.02 nPa, a moderate $B_{SW} \sim 0.3$ nT and small reconnection potential drop, $\Phi \sim 30$ kV, which caused the auroral oval to move to higher latitudes and became more intense, 5.) A second shock related feature (S2) when a CIR shock was observed upstream by Cassini which had a high solar wind ram pressure, $P_{SW} \sim 0.05$ nPa , high magnetic field strength, $B_{SW} \sim$ 2 nT, and a high reconnection potential, $\Phi \sim 300$ kV, which caused the aurora to become very intense toward dawn and filled the auroral oval toward Saturn's pole on the dawn side, and 6.) A relaxation (R) period that occurred after S2, when the oval moved to

lower latitudes and the intensity decreased to moderate. The general morphology shows a spiral pattern that moves from $\lambda \sim 72°$ at dawn, to $\lambda \sim 75°$ at noon to $\lambda \sim 70°$ at dusk. The intensity decreases as one goes from dawn, to noon and then dusk. Near midnight the structure and intensity are uncertain because of poor viewing from the Earth. Most of these features can be explained by our model in a qualitative sense.

Jupiter has three main components in its auroral display (see *Clarke et al. [2004],* for a recent and comprehensive review). At lower latitudes, three bright spots have been clearly identified as the magnetic projections of the satellites Io, Ganymede and Callisto. At higher latitudes, auroral forms are diffuse, complex and highly variable. They seem to relate in a complicated way to the Dungey and Vasyliunas cycles of magnetospheric convection. The main oval between these two regions and is the brightest source. It corotates with Jupiter and in response to changes in the upstream solar wind conditions displays a limited brightness variation but no position variation.

Reconnection Model

Cowley et al. [2004a,b], proposed a steady state model of Saturn's aurora and flows in the outer magnetosphere to explain the auroral observations. They postulated reconnection on the dayside magnetopause with corresponding addition of open magnetic flux to the outer magnetosphere, which they refer to as Dungey-cycle flow. Regions of closed field line flows outside $L \sim 15$ move radially outward between noon local time and dusk local time. The field lines become stretched out in the midnight-dusk sector and

reconnection occurs, ejecting plasmoids down the tail. The rotation of the magnetosphere then transports the reconnected closed field lines, which are loaded with hot plasma from the reconnection process, to the midnight and dawn local times of the outer magnetosphere. They refer to this region as the Vasyliunas-cycle flow region; this flow cycle was proposed by *Vasyliunas [1983]* for Jupiter's magnetosphere. In their model, compression of the magnetosphere results in reconnection of the open flux in the tail lobes in the vicinity of the Vasyliunas-cycle flow region in the magnetotail. This reconnection results in the injection of hot plasma and enhanced precipitation into Saturn's ionosphere with corresponding auroral brightening. Rotation then convects this plasma to the dawn side and produces the spiral structure reported by *Clarke et al. [2005]*.

Similar flow cycles should operate in Jupiter's magnetosphere. Voyager 2 observed a magnetospheric wind of hot plasma within the core regions of Jupiter's distant magnetotail at distances ~ 5000 R_J down the tail *[Sittler et al., 1987]*. This magnetospheric wind was likely composed of a heavy ion component (i.e., O^+/S^{++}), had a temperature T ~ 87 keV and moved down the tail with speed V ~ 200 km/s. This magnetospheric wind appears to always be present. Therefore, reconnection in the near Jovian tail, r ~ 150 R_J, is always going on and results in no change in the main auroral oval topology. When plasmoid formation occurs at Jupiter, there is no return flow from the tail to Jupiter's inner magnetosphere where the aurora is being produced. If the same hold for Saturn, then reconnection in the tail would not map to Saturn's aurora and the

bulk of the hot plasma escapes down the tail as a magnetospheric wind [see Vasyliunas, 1975].

Centrifugal Instability Model

We propose an alternative model, shown in Figure 4, following the arguments by *Goertz [1983]* who presented a model that could explain the sharp outer boundary of Saturn's plasma sheet and the formation of plasma islands or 'blobs of plasma'. As the plasma moved along the dawn flank of the magnetosphere a Kelvin-Helmholtz instability could take place. When combined with a centrifugal instability of the flux tubes, the plasma and field would be highly turbulent in this region of the magnetosphere and caused islands of plasma to break off from the plasma sheet outer boundary as observed. Taking this idea one step further, we argue that when a CIR encounters Saturn's magnetosphere, the Kelvin-Helmholtz instability is enhanced on the dawn-side causing more turbulence, heating of the plasma, enhanced outward radial transport via the centrifugal flux tube instability and thus a brightening of the aurora on the dawn side and movement of the auroral oval to higher latitudes as observed.

We adopt the model by *Curtis et al., [1986]* for SKR generation. The plasma sheet outer boundary steepens on the dayside and is more unstable to the centrifugal flute instability, which leads to the formation of plasma islands. MHD instabilities or surface waves are generated along the magnetic field lines threading the detached plasma islands. These waves mode convert into kinetic Alfvèn waves [*Hasegawa*, 1976]. The kinetic Alfvèn

waves can then form field-aligned potential drops ~ several kV and accelerate electrons along the magnetic field to produce the aurora and SKR emissions. This model requires a reservoir of keV electrons in order to work. *Curtis et al. [1986]* argue, similar to *Goertz* [1983], that islands of disconnected field lines will move radially outward to r ~ 30 R_S on the night side and disconnect, forming a planetary wind down the tail. When this happens, the reservoir of keV electrons are lost down the tail and the density gradients are weakened, which then make the flux tubes more stable against the centrifugal flute instability. Thus SKR is not observed on the nightside. After disconnection, the flux tubes rotate to dawn and then noon, and start to fill up with hot pickup of ions formed from the ionization of the resident neutral clouds in the outer magnetosphere *[see Sittler et al., 2004 and Johnson et al., 2005]*. The pickup process also heats the electrons to a few keV *[Barbosa, 1987],* which replenishes the reservoir of keV electrons needed for the mechanism by *Hasegawa* [1976] to further accelerate the keV electrons via kinetic Alfven waves along the magnetic field and produce the observed aurora and SKR emissions. This process is amplified when the magnetosphere is compressed (i.e., compression of magnetosphere on dayside and enhanced elongation of nightside field lines). This mechanism accounts for the correlation between auroral brightening and SKR enhancements and for the concentration of SKR emission near noon [*Kurth et al.*, 2005]. Therefore, our model also provides a mechanism for the correlation between auroral brightening and SKR intensification. The higher density flux tubes in Saturn's plasma sheet contain a mix of hot and cold plasma *[Sittler et al., 1983], thus the hot keV plasma which refills the flux tubes must mix with the outward moving cold plasma from the inner magnetosphere.*

We present evidence that as the magnetosphere is compressed, conservation of angular momentum causes the magnetosphere to spin up. This spin up increases the rate of centrifugally driven radial transport, which moves the turbulent-hot plasma radially outward where it maps to auroral field lines at higher latitudes. This model gives a natural explanation for the intensification of the auroral emissions along the dawn meridian and its movement to higher latitudes. The turbulent nature of the mechanism can also explain the observed patchiness of the aurora, especially during time periods of auroral intensification.

MODEL

We present a relatively simple explanation for Saturn's observed auroral response to a compression region in the solar wind. It is directly based on the fact that it is a fast rotator with a weak coupling to the ionosphere, in which a change in the rotation state of the plasmasphere will induce a change in radial transport and ionosphere/magnetosphere coupling currents.

Compression of the magnetosphere and changes in the rotation state

The magnetosphere, in a global sense, will tend to conserve angular momentum; when compressed, if the torques on the system are relatively small, this effect will cause the rotating flow to spin up. The plasma observations [*Lazarus and McNutt, 1983; Richardson, 1986; Eviatar et al., 1983*] indicate that Saturn's ionospheric height

integrated Pedersen conductivity is not sufficiently large to enforce co-rotation in the outer magnetosphere, which implies that the associated poloidal current system and its corresponding torque on the system is relatively small. To first order, compression of the dayside magnetosphere gives radially inward motion, so that the torque on the magnetosphere $\vec{\tau} = \vec{r} \times \vec{F}_r \sim 0$, ($F_r$ symbolizes a radial force) with its angular momentum approximately conserved. In the boundary layer, this condition might be violated, but for the global magnetospheric response this should be correct. Further evidence for a torque free response are the small values for the toroidal magnetic field $B_\phi \sim \pm 1$ nT [*Smith et al., 1980a; Connerney et al., 1983*] in the dayside outer magnetosphere. The small B_ϕ suggests that field aligned currents needed to enforce co-rotation are small (i.e., height integrated Pedersen conductivity $\Sigma_P \sim 0.2$ mho *[Eviatar et al., 1983]*) and the magnetospheric response is essentially torque free. We do note, that $\Sigma_P \sim$ 1-2 mho have been reported at lower ionospheric latitudes where they map to Saturn's inner magnetosphere [*Bunce et al., 2003*], but could also be due to field-aligned currents in the polar regions [*Connerney et al., 1983*]. If we compare the dimensions of the magnetosphere before and after compression, using Pioneer 11 as an example, we estimate that $\Omega \sim (\Omega_{cor}/2)(21/17)^2 \sim 75\%$ (where $\Omega_{cor}/2$ is the normal rotation rate in the outer dayside magnetosphere). This value is consistent with the HST observations reported by *Clarke et al. [2005]* (Here, we note that the actual spinning up of the aurora is not directly observed, but only inferred).

Changes in rotation rate and their effects on radial transport

If radial transport is dominated by centrifugally driven flux tube interchange motions [*Siscoe and Summers*, *1981; Southwood and Kivelson,1987; André and Ferrière*, *200x*; *Ferrière et al. [1999, 2001]*] then the magnetosphere spin up enhances the transport with transport time scale $T_L \propto \Sigma_P/\Omega^2 \sim 5$ hours (where $\Sigma_P \sim 0.2$ mho [*Eviatar et al*., *1983*]; mass loading rate, $dNL^2/dL \sim 5x10^{32}$ [*Richardson et al.*, *1998*] and eddy size $\Delta L \sim 0.41$ R_S [*Lepping et al.*, *2005*] at outer boundary of plasma sheet). If, however, Σ_P is enhanced by the auroral brightening, this will counter the increase in outward radial transport due to spinning up of the magnetospheric plasma. In order to do this calculation correctly we may need to use the approach by *Goertz [1983],* which considered the detachment of eddies from the plasma sheet outer boundary. In that model the time scales for movement of these eddies or islands to the magnetopause or ejection down the tail was suggested to ~ a few rotation periods, but no specific calculations were given. When the rotating plasma moves from the dayside to the night side the field lines are expected to move out to larger radial distances and near the equatorial plane they could become extended *[Goertz, 1983]*. Here, the plasma may merge with the tail plasma sheet in a rather complex fashion, which is beyond the scope of this paper.

After passage of a compression region, rarefraction regions are common. Rarefractions cause the magnetosphere to expand, reducing the angular velocity of the rotating flow and the outward transport rate and causing the auroral oval to move to lower latitudes. This is contrary to that observed at Earth. Figures 1, 2 and 3 show the plasma flow characteristics observed by Voyager [*Richardson*, 1986]; the rotational speed V_ϕ and the radial outflow V_R are anti-correlated (i.e., $V_R > 0$ for expanding magnetosphere and $V_R <$

0 for compression of magnetosphere). The radial component of the flow is needed to determine whether the magnetosphere is undergoing compression or expansion and whether the azimuthal flow conserves angular momentum for a particular flux tube. With regard to the passage of a rarefraction region, we note that the Voyager 2 outbound observations reported by *Sittler et al. [1983],* showed that the plasma sheet along the dawn flank was observed all the way to the magnetopause at L ~ 25. During this time it was believed that Saturn may be within Jupiter's distant magnetotail and that external pressures were low. Following arguments by *Curtis et al. [1986],* under these conditions the plasma sheet outer boundary would not be compressed and thus more stable against the centrifugal flute instability as observed.

Recently, Sittler et al. [2005] have presented fluid parameters derived from the Cassini plasma instrument, and found that V_ϕ and V_R were anti-correlated in Saturn's inner magnetosphere for L < 8.5. They also show a gradual increase in $V_R > 0$ with distance, which is consistent with outward radial transport. Outside Dione at L = 6.3, the plasma starts to sub-corotate. Injection events were observed, in which regions of hot plasma, low density plasma with $V_R < 0$ have moved from the outer to the inner magnetosphere [Burch et al., 2005; Young et al., 2005; Sittler et al., 2005].

Relation to auroral electron precipitation

One of the key elements of any model of Saturn's aurora are the energy flux and pitch angle distribution of the precipitating particle populations along with their space and time

dependences within the magnetosphere. These properties are especially important for our model, in which the precipitating particles originate at the outer boundary of Saturn's inner plasmasphere. Our model requires a negative radial gradient in the electron energy flux in order to account for the movement of auroral features to higher latitudes as these islands of plasma move radially outward. It is also important to demonstrate that the precipitating particles are magnetically connected to the observed auroral features. It is believed that keV electrons are primarily responsible for Saturn's aurora [G*èrard et al.,* 2004].

Figure 5 shows the electron energy flux incident on Saturn's ionosphere as a function of radial distance derived from Voyager 1 and 2 PLS and LECP electron observations [*Maurice et al.*, 1996]. We show Voyager 1 electron energy fluxes for energies < 200 keV and Voyager 2 electron energy flux for 200 keV < E < 1 MeV. The Voyager 2 data intensities are not expected to produce significant excitation of Saturn's aurora. The mean energy of the electrons exciting the aurora is ~ 12 keV [*Clarke et al.*, 2005; *Gèrard et al.*, 2004]. The energy flux, assuming full downward loss cone, is plotted as a function of co-latitude at the top of Saturn's ionosphere for both the north and south polar regions, using the internal magnetic field model with ring current by *Connerney et al.*, [1981, 1982]. For a co-latitude $\theta \sim 18°$, the center of the auroral oval in the south polar regions [see Cowley and Bunce, 2003; Cowley et al., 2004; Gèrard et al., 2004], the field lines map to an equatorial radius of $r \sim 15\ R_S$, which is approximately the outer boundary of the dayside plasma sheet and outer boundary of the ring current [*Connerney et al.*, 1983]. Figure 6 shows the field line mapping from Saturn's ionosphere to the equatorial plane. The

auroral emissions are observed in a band between 10° and 20° in co-latitude; since magnetospheric dimensions vary with local time, field line mapping has considerable uncertainties. This region also has enhanced levels of ion cyclotron waves [*Lepping et al.*, 2005], which can pitch angle scatter keV heavy ions and energetic protons with E ~ 200 keV [*Sittler et al.*, 2004]. *Barbosa [1987]* argued that pickup ions in the outer magnetosphere can accelerate electrons along field lines to keV energies (giving pitch angle distributions for keV electrons with $T_{ll}/T_{\perp} >> 1$ are predicted) via lower hybrid electrostatic waves with electric fields $\delta E \sim 0.1$ mV/m at a frequency $\nu_{LH} \sim 1$ Hz. Frequencies $\nu_{LH} \sim 1$ Hz are below the detection threshold of the Voyager plasma wave receiver, which may account for the lack of detection of the lower hybrid waves. Similar to the ion cyclotron waves, these higher frequency lower hybrid electrostatic waves could enhance the precipitation of electrons near the turbulent outer boundary of the plasma sheet [*Sittler et al.*, *1983*; *Sittler et al., 2004*; *Lepping et al.*, *2005*]. Furthermore, as proposed by *Curtis et al. [1986],* the centrifugal flute instability can cause MHD instabilities that can mode convert into kinetic Alfven waves and accelerate electrons with energies ~ several keV along the magnetic field. So, it is not unreasonable to expect $T_{ll} / T_{\perp} >> 1$ for the keV electrons at the outer boundary of the plasma sheet and in the detached plasma islands.

Although, electron pitch angle distributions at the plasma sheet outer boundary have not yet been reported, we expect on theoretical grounds that the loss cone will be filled. The intensity of the electron energy flux may then be sufficient to produce the diffuse aurora (i.e., region "O" defined in *Grodent et al*., 2005), and possibly the intense auroras

observed during storms [*Clarke et al.*, 2005] with energy fluxes ~ 3-5 mW/m^2 at λ_{SH} ~ 72° (i.e., 30-50 krad, see Cowley et al. [2004a] for conversion factor). In the inner magnetosphere, in contrast, pitch angle scattering is weak so precipitating electron fluxes are small and auroral emission is weak [*Scarf et al.,* 1984]. The analysis by *Scarf et al.* [1984] was based on Voyager 1 data acquired during the equatorial crossing of Dione's L shell where whistler mode waves were observed and a trapped electron population with $T_\perp / T_{ll} > 1$ was inferred. In addition to the other mechanisms which produce hot electrons, we may require field aligned potential drops above Saturn's ionosphere, similar to that for Jupiter's aurora [*Cowley et al.*, 2003], to produce the observed auroras at Saturn. If field aligned potential drops ~ several kV did form, they would be at heights within a few R_S of the ionosphere, where the corresponding field-aligned currents probably would not produce observable toroidal magnetic fields in the outer magnetosphere and thus not violate observations.

In the inner magnetosphere, *Connerney et al.*, [1983] reported a significant toroidal field component in the Voyager 1 magnetometer data, which they attributed to a large field-aligned current system in the southern polar region, close to Saturn. These observations indicate that large field-aligned electric fields can form close to the planet and enhance the auroral emissions [*Cowley et al.*, 2003]. The presence of large field aligned potential drops at high latitudes is also supported by recent observations [*Kurth et al.,* 2005] that SKR emissions drop to lower frequencies, ~ 100 kHz, when they become most intense. Since the emissions are expected to occur near the electron gyro-frequency, the source

region must move to higher altitudes as the emission intensifies which suggests that large the field aligned potential drops are forming at higher altitudes [see Knight, 1973].

Following the arguments by *Goertz [1983]*, the Kelvin-Helmholtz instability will be enhanced on the dawn-side where the velocity shear across the magnetopause is the greatest. When a CIR encounters Saturn's magnetosphere, the velocity shear boundary will move inward and be enhanced (since the magnetosphere spins up), causing more turbulence, heating the plasma, and enhanced outward radial transport via the centrifugal flute instability [see *Curtis et al., 1986*]. Also, when the magnetosphere is compressed, the plasma will be energized by betatron acceleration due to conservation of the first and second adiabatic invariants. These effects result in brightening of the aurora on the dawn side and movement of the aurora emission to higher latitudes, as observed. So, under these conditions we may have time dependent pitch angle scattering toward the strong diffusion limit and provide the required precipitating energy flux needed to produce the observed auroral brightening. The model is not yet mature enough to provide quantitative estimates, but does seem plausible in a qualitative sense.

Preliminary model predictions

Our model is based on data acquired during brief encounters with Saturn's magnetosphere by Pioneer 11, Voyager 1 and Voyager 2 (i.e., snap shots in time) and the limited observations of Saturn's aurora by HST. The four years of Cassini observations of the Kronian magnetosphere will progressively provide more complete coverage of all the

main plasma and field domains, including the high latitudes and the tail regions. Our model makes the following predictions which will be tested by Cassini:

- The azimuthal and radial velocities in the dayside outer magnetosphere will be anti-correlated.
- During times of large azimuthal velocities and large negative radial velocities within the dayside outer magnetosphere, the auroral brightness will increase and the SKR will intensify.
- During periods of auroral brightening or enhanced SKR, the turbulence of the plasma on the dawn side of the magnetosphere will increase and the velocity shear boundary of the magnetopause will move inward.
- Within regions of enhanced turbulence the plasma will be heated and enhanced wave activity will be observed by the plasma wave and magnetometer instruments. The electron pitch angle distributions will be more dumbbell like. Betatron acceleration is also expected to be important.
- Between dusk and midnight in the outer magnetosphere flux tubes will move to larger radial distances with increasing local time. The plasma sheet outer boundary will move farther out with increasing local time, the radial velocity of the flow will increase to more positive values and the azimuthal velocity will decrease.
- The islands of enhanced plasma density within the magnetotail will become disconnected from the planetary field and form plasmoids that are ejected down the tail as a magnetospheric wind.

- The closed flux tubes to smaller radial distances as they move from midnight to dawn local time, with an increase in turbulence toward dawn local time in the outer magnetosphere. The radial velocities will be more negative and the azimuthal velocities will increase as the flux tubes move toward dawn.
- We should look for evidence of field aligned potential drops during the polar orbital phase of the mission, especially along the dawn meridian. The alignment of the high inclination passes is along the dawn-dusk meridian.
- During times when $\delta V_R > 0$ and $\delta V_\phi < 0$, the ionosphere coupling will result in $\delta B_\phi < 0$. For $\delta V_R < 0$ and $\delta V_\phi > 0$, $\delta B_\phi > 0$ (δB_ϕ flips sign at the magnetic equator, we refer here to latitudes above the magnetic equator). This B_ϕ affect may be complicated by the expansion and compression of Saturn's magnetosphere as the external pressure of the solar wind varies.

SUMMARY

We developed the centrifugal instability model to explain the relationship between the HST auroral observations [*Clarke et al.*, *2005*] and the Cassini upstream solar wind observations [*Crary et al.*, *2005*]. Saturn's magnetosphere is a fast rotator and the ionosphere cannot enforce corotation in the outer magnetosphere [*Lazarus and McNutt*, 1983; *Richardson*, 1986; *Eviatar et al.*, 1983]. Thus, the torques on the system are sufficiently small that the magnetosphere will tend to conserve angular momentum during periods of changing external pressure. The small values of B_ϕ observed in the

outer magnetosphere [*Smith et al.*, 1980a; *Connerney et al.,* 1983] are consistent with the torques being small. Therefore the flow is essentially torque free with angular velocity $\Omega \propto 1/r^2$. During periods of compression the rotating flow will spin up, and during periods of expansion it will spin down. We showed a case study of a compression event in which the outer magnetosphere spun up from $\Omega \sim \Omega_{cor}/2$ to ~ 75% of Ω_{cor} which can be inferred from the HST observations reported by *Clarke et al.*, [2005]. Since the time scale for centrifugally driven flux tube interchange motions $T_E \propto \Sigma_P/\Omega^2 \sim 5$ hours, outward radial transport is enhanced when the magnetosphere spins up and flux tubes will move outward. This outward motion moves the auroral oval to higher latitudes during times of increased solar wind pressure as observed [*Clarke et al.*, 2005]. The precipitating particles reside in the outer magnetosphere, near the outer boundary of the plasma sheet and ring current, where the plasma is highly turbulent and has enhanced ion cyclotron wave activity [*Sittler et al., 2004; Lepping et al., 2005*]. We suggest that this model may account for the observed drift in clock frequency of the Saturn Kilometric Radiation (SKR) [*Galopeau and Lecacheux,* 2000], which plays a very important role with regard to measuring the rotation rate of the planet [*Galopeau and Lecacheux*, 2000]. As discussed in *Curtis et al. [1986],* this model also provides a natural explanation of the SKR, its correlation with auroral brightening and its primary occurrence on the dayside magnetosphere.

This model, as well as the competing model of *Cowley et al.* [2005], is derived from a limited set observations. Future studies should consider the whole range of solar wind parameters, particularly IMF orientation whose effects were not considered here. In this

context, we note that the dipole moment, aligned with Saturn's spin axis, is tilted by 27° away from the Sun and along the Sun-Saturn line at the time of the Cassini Saturn Orbit Insertion (SOI). Then as the Cassini tour progresses, and Saturn orbits around the Sun (i.e., 29 year orbital period), the dipole axis will be tilted orthogonal to the Sun-Saturn line. At r ~ 9.5 AU, the average interplanetary field is orthogonal to the flow direction of the solar wind, and for a two sector configuration for the heliospheric field, the field polarity would not change for time periods ~ 12 days. Therefore, similar to the B_y effect for Earth [*Holzer and Slavin, 1982; Russell and McPherron, 1973*], one could have reconnection on the frontside of Saturn's magnetosphere for periods ~ 12 days (positive polarity for interplanetary field) and then when a sector boundary occurs, have time periods ~ 12 days when the magnetosphere is closed (negative polarity for interplanetary field). So, by the end of Cassini's extended mission (~ 6 years), this effect will have maximized and one could have long periods of high activity and long periods of low activity for Saturn's magnetosphere and its aurora.

Our model is different from that proposed by *Cowley et al. [2004c],* in that they heat the plasma via compression-induced reconnection of the open magnetic flux in the tail lobes in the Vasyliunas-cycle flow region, which was originally proposed by *Vasyliunas [1983]* for Jupiter's magnetosphere. Our explanation for auroral brightening on the dawn side and movement of the aurora to higher latitudes follows the argument by *Goertz [1983]* with regard to the formation of detached plasma islands at the plasma sheet outer boundary. The detachment of plasma may preferably occur on the dawn side of the magnetosphere where the Kelvin-Helmholtz instability would be most important, because

of the large velocity shear at the dawn magnetopause. When a CIR encounters Saturn's magnetosphere, the velocity shear boundary on the dawn side will be enhanced and move inward, causing more turbulence, heating of the plasma, and an increased outward radial transport via the centrifugal flute instability [see *Curtis et al., 1986*]. This effect is enhanced by the fact that field lines loaded with islands of plasma will move outward as they rotate from dusk to midnight, where the confining effects of the solar wind are minimal, and be lost via a planetary wind. This will then result in a sharpened outer boundary of the plasma sheet now devoid of hot plasma. Then as the plasma rotates toward dawn hot plasma will accumulate via pickup ions from ionization of neutral clouds in the outer magnetosphere [see *Sittler et al., 2004 and Johnson et al., 2005*]. Since the outer boundary of the plasma sheet is outside r ~ 20 R_S, this plasma will be closer to the magnetopause on the dawn side in an average sense. Combining the above facts we would then expect a brightening of the aurora on the dawn side and its movement to higher latitudes as observed. This effect will be enhanced during passage of a CIR.

For our model, the source of the precipitating particles which produce the aurora are, 1.) the pickup of ions at keV energies in the outer magnetosphere due to the ionization of the neutral clouds which extend beyond Titan's orbit [Sittler et al., 2004; Johnson et al., 2005], 2.) the pickup process results in an ion beam instability which accelerates electrons along the magnetic field with keV energies via lower-hybrid waves [*Barbosa,* 1987], 3.) the centrifugal flute instability produces MHD wave instabilities such as kinetic Alfven waves and further accelerates the reservoir of hot electrons from the

pickup process to keV energies [*Curtis et al.,* 1986] and 4.) the above processes are enhanced near dawn where the Kevin-Helmholtz instability is strongest and toward noon where the plasma sheet outer boundary may steepen radially which can enhance the centrifugal flute instability which produces plasma islands [*Curtis et al.*, 1986]. The above processes will always present, but are enhanced when the magnetosphere is compressed during the passage of a CIR.

REFERENCES

Barbosa, D. D., Titan's atomic nitrogen torus: Inferred properties and consequences for the Saturnian aurora, (1987), *Icarus*, *72*, 53.

Blanc, M., R. Kallenbach and N.V. Erkaev, (2004), Solar System Magnetospheres, *The Outer Planets, A Comparative Study before the Exploration of Saturn by Cassini-Huygens,* Editors, T. Encrenaz, R. Kallenbach, T. C. Owen, C. Sotin, 227.

Bunce, E. J., S. W. H. Cowley and J. A. Wild, (2003), Azimuthal magnetic fields in Saturn's magnetosphere: effects associated with plasma sub-corotation and the magnetopause-tail current system, *Ann. Geophys.*, *21*, 1709-1722.

Bridge, H. S., J. W. Belcher, A. J. Lazarus, J. D. Sullivan, R. L. McNutt, F. Bagenal, J. D. Scudder, E. C. Sittler Jr., G. L. Siscoe, V. M. Vasyliunas, C. K. Goertz and C. M. Yeates, (1979), Plasma observations near Jupiter: Initial results from Voyager 1, *Science*, **204**, 987.

Bridge, H. S., J. W. Belcher, A. J. Lazarus, S. Olbert, J. D. Sullivan, F. Bagenal, P. R. Gazis, R. E. Hartle, K. W. Ogilvie, J. D. Scudder, E. C. Sittler, A. Eviatar, G. L. Siscoe,

C. K. Goertz and V. M. Vasyliunas (1981), Plasma observations near Saturn: Initial results from Voyager 1, *Science*, *80*, 217.

Bridge, H. S., F. Bagenal, J. W. Belcher, A. J. Lazarus, R. L. McNutt, J. D. Sullivan, P. R. Gazis, R. E. Hartle, K. W. Ogilvie, J. D. Scudder, E. C. Sittler, A. Eviatar, G. L. Siscoe, C. K. Goertz and V. M. Vasyliunas (1982), Plasma observations near Saturn: Initial results from Voyager 2, *Science*, *215*, 563.

Burch, J. L., J. Goldstein, T.W. Hill, D.T. Young, F.J. Crary, A.J. Coates, N. Andre, W.S. Kurth and E.C. Sittler, Jr., Properties of local plasma injections in Saturn's magnetosphere, (2005), *Geophys. Res. Lett.*, **32**, No. 14, L14S02, 10.1029/2005GL022611.

Clarke, J., J.-C. Gerard, D. Grodent, S. Wannawichian, J. Gustin, J. Connerney, F. Crary, M. K. Dougherty, W. Kurth, S. W. H. Cowley, E. J. Bunce and T. W. Hill, (2005), Morphological differences between Saturn's ultraviolet aurorae and those of Earth and Jupiter, *Nature*, **433**, 717.

Clarke, J. T., D. Grodent, S. W. H. Cowley, E. J. Bunce, P. Zarka, J. E. P. Connerney and T. Satoh, (2005), Jupiter's Aurora, *Jupiter*, editor, F. Bagenal, 2004.

Connerney, J.E.P., M. H. Acuna, and N. F. Ness, (1981), Saturn's ring current and inner magnetosphere, *Nature*, *292*, 724.

Connerney, J.E.P., N. F. Ness and M.H. Acuna, (1982), Zonal harmonic model of Saturn's magnetic field from Voyager 1 and 2 observations, *Nature*, *298*, 44.

Connerney, J. E. P., M. H. Acuna and N. F. Ness, (1983), Currents in Saturn's magnetosphere, *J. Geophys. Res.*, *88*, 8779.

Cowley, S.W.H., E.J. Bunce and J.D. Nichols, (2003), Origins of Jupiter's main oval auroral emissions, *J. Geophys. Res.*, *108*(A4), 8002, doi:10.1029/2002JA009329.

Cowley, S. W. H. and E. J. Bunce, (2003), Corotation-driven magnetosphere-ionosphere coupling currents in Saturn's magnetosphere and their relation to the auroras, *Ann. Geophys.*, **21**, 1691-1707.

Cowley, S. W. H., E. J. Bunce and R. Prange, (2004a), Saturn's polar ionospheric flows and their relation to the main auroral oval, *Ann. Geophys., 22,* 1379.

Cowley, S. W. H., E. J. Bunce and J. M. O'Rourke, (2004b), A simple quantitative model of plasma flows and currents in Saturn's polar ionosphere, *J. Geophys. Res.*, *109*, (A05212), doi:10.1029/2003JA010375.

Cowley, S. W. H., S. V. Badman, E. J. Bunce, J. T. Clarke, J. –C. Gerard, D. Grodent, C. M. Jackman, S. E. Milan and T. K. Yeoman, (2005), Reconnection in a rotation-dominated magnetosphere and its relation to Saturn's auroral dynamics, *J. Geophys. Res.*, **110**, A02201, doi:10.1029/2004JA010796.

Crary, F., J. T. Clarke, M. K. Dougherty, P. Hanlon, K. C. Hansen, J. Steinberg, B. Barraclough, A. J. Coates, J.-C. Gerard, D. Grodent, W.S. Kurth, D. G. Mitchell, A. M. Rymer and D. T. Young, (2005), Solar wind dynamic pressure and electric field as the main factors controlling Saturn's aurorae, *Nature,* **433**, 720.

Curtis, S. A., R. P. Lepping, and E. C. Sittler, Jr., The centrifugal flute instability and the generation of Saturn kilometric radiation, *J.Geophys. Res.*, **91**, 10,989-10,994, 1986.

Elphinstone, R. D., J. S. Murphree and L. L. Coggar, (1996), What is a global auroral substorm?, *Reviews of Geophysics*, *34*, 169-232.

Eviatar, A., R.L. McNutt, Jr., G.L. Siscoe and J.D. Sullivan, (1983), Heavy ions in the outer Kronian magnetosphere, *J. Geophys. Res.*, *88*, 823-831.

Ferriere, K.M., C. Zimmer and M. Blanc, (1999), Magnetohydrodynamic waves and gravitational/centrifugal instability in rotating systems, *J. Geophys. Res.*, **104**, 17335-17356.

Ferriere, K. M., C. Zimmer and M. Blanc, (2001), Quasi-interchange modes and interchange instability in rotating magnetosphere, *J. Geophys. Res.*, **106**, 327-344.

Frank, L. A., B. G. Burek, K. L. Ackerson, J. H. Wolfe, and J. D. Mihalov, (1980), Plasmas in Saturn's magnetosphere, *J. Geophys. Res.*, *85*, 5695.

Galopeau, P. H. M., and A. Lecacheux, (2000), Variations of Saturn's radio rotation period measured at kilometer wavelengths, *J. Geophys. Res.*, *105*(A6), 13089-13101.

Gerard, J.-C., D. Grodent, J. Gustin, A. Saglam, J. T. Clarke and J. T. Trauger, (2004), Characteristics of Saturn's FUV aurora observed with Space Telescope Imaging Spectrograph, *J. Geophys. Res.*, *109*, doi:10.1029/2004JA010513.

Goertz, C. K., (1983), Detached plasma in Saturn's fron side magnetosphere, *Geophys. Res. Lett.*, *10*(6), 455-458.

Grodent, D., J. –C. Gèrard, S. W. H. Cowley, E. J. Bunce and J. T. Clarke, (2005), Variable morphology of Saturn's southern ultraviolet aurora, *J. Geophys. Res.*, **110**, A07215, doi:10.1029/2004JA010983.

Hasegawa, A., (1976), Particle acceleration by MHD surface wave and formation of aurora, *J. Geophys. Res.*, **81**, 5083.

Holzer, R. E. and J. A. Slavin, (1978), Magnetic flux transfer associated with expansions and contractions of the dayside magnetosphere, *J. Geophys. Res.*, **83**, 3831.

Holzer, R. E. and J. A. Slavin, (1982), A quantitative model of geomagnetic activity, *J. Geophys. Res.*, **87**, 9054.

Johnson, R. E., M. Liu and E. C. Sittler Jr., (2005), Plasma-induced clearing and redistribution of material embedded in planetary magnetospheres, *Geophys. Res. Lett.*, **32**, L24201, doi:10.1029/2005GL024275.

Knight, S., Parallel electric fields, *Planet. Space Sci.,***21**, 741, 1973.

Kurth, W. S., D. A. Gurnett, J. T. Clarke, M. D. Desch, M. L. Kaiser, P. Zarka, B. Cecconi, A. Lecacheux, W. M. Farrell, P. Galopeau, J. –C. Gerard, D. Grodent, M. K. Dougherty, F. J. Crary and R. Prange, (2005), An Earth-like correspondence between Saturn's auroral features and radio emission, *Nature*, **433**, 722.

Lazarus, A. J. and R. L. McNutt Jr., (1983), Low-energy plasma ion observations in Saturn's magnetosphere, *J. Geophys. Res.*, *88*, 8831.

Lepping, R.P., E. C. Sittler, Jr., W. H. Mish, S.A. Curtis and B.T. Tsurutani, (2005), Analysis of waves in Saturn's magnetosphere: Voyager 1 observations, *J. Geophys. Res.*, **110**, A05201, doi:10.1029/2004JA010559.

Maurice, S., E. C. Sittler Jr., J. F. Cooper, B. H. Mauk, M. Blanc, and R. S. Selesnick, (1996), Comprehensive analysis of electron observations at Saturn: Voyager 1 and 2, *J. Geophys. Res.*, *101*, 15211.

Ness, N. F., M. H. Acuna, R. P. Lepping, J. E. P. Connerney, K. W. Behannon, L. F. Burlaga and F. M. Neubauer, (1981), Magnetic field studies by Voyager 1: Preliminary results at Saturn, *Science*, *212*, 211.

Ness, N. F., M. H. Acuna, K. W. Behannon, L. F. Burlaga, and F. M. Neubauer, (1982), Magnetic field studies by Voyager 2: Preliminary results at Saturn, *Science*, *215*, 558.

Reiff, P. H., R. W. Spiro and T. W. Hill, (1981), Dependence of polar cap potential drop on interplanetary parameters, *J. Geophys. Res.*, **86**, 7639.

Richardson, J. D., (1986), Thermal ions at Saturn: Plasma parameters and implications, *J. Geophys. Res.*, *91*, 1381.

Richardson, J. D. and E. C. Sittler, Jr., (1990), A plasma density model for Saturn based on Voyager observations, *J. Geophys. Res.*, *95*, 12019.

Richardson, J.D., A. Eviatar, M.A. McGrath and V.M. Vasyliunas, (1998), OH in Saturn's magnetosphere: Observations and Implications, *J. Geophys. Res., 103*, 20245.

Russell, C. T. and R. L. McPherron, (1973), The semi-annual variation of geomagnetic activity, *J. Geophys. Res.*, **78**, 92.

Scarf, F.L., L.A. Frank, D.A. Gurnett, L.J. Lanzerotti, A. Lazarus and E.C. Sittler Jr., (1984), Measurements of plasma, plasma waves and suprathermal charged particles in Saturn's inner magnetosphere, *Saturn*, University of Arizona Press, 318.

Siscoe, G.L. and D. Summers, (1981), Centrifugally driven diffusion of Iogenic plasma, *J. Geophys. Res.*, *86*, 8471-8479.

Sittler, E. C., Jr., K. W. Ogilvie and J. D. Scudder, (1983), Survey of low-energy plasma electrons in Saturn's magnetosphere: Voyagers 1 and 2, *J. Geophys. Res.*, *88*, 8847.

Sittler, E. C., Jr., R. P. Lepping, B. H. Mauk and S. M. Krimigis, (1987), Detection of a hot plasma component within the core regions of Jupiter's distant magnetotail, *J. Geophys. Res., 92*, 9943.

Sittler, E. C., Jr., R. E. Johnson, H. T. Smith, J. D. Richardson, S. Jurac, M. Moore, J. F. Cooper, B. H. Mauk, M. Michael, C. Paranicas, T. P. Armstrong and B. T. Tsurutani,

(2004), Energetic nitrogen ions within the inner magnetosphere of Saturn, *J. Geophys. Res.*, in review.

Sittler, E. C., Jr., M. Thomsen, D. Chornay, M. D. Shappirio, D. Simpson, R. E. Johnson, H. T. Smith, A. J. Coates, A. M. Rymer, F. Crary, D. J. McComas, D. T. Young, D. Reisenfeld, M. Dougherty and N. Andre, (2005), Preliminary results on Saturn's inner plasmasphere as observed by Cassini: Comparison with Voyager, *Geophys. Res. Lett.*, **32**, L14S07, doi:10.1029/2005GL022653.

Slavin, J. A., E. J. Smith, P. R. Gazis and J. D. Mihalov, (1983), A Pioneer-Voyager study of the solar wind interaction with Saturn, *Geophys. Res. Lett.*, **10(1)**, 9.

Smith, E. J., L. Davis, D. E. Jones, P. J. Coleman Jr., D. S. Colburn, P. Dyal and C. P. Sonett, (1980a), Saturn's magnetic field and magnetosphere, *Science*, *207*, 407.

Smith, E. J., L. Davis, D. E. Jones, P. J. Coleman Jr., D. S. Colburn, P. Dyal and C. P. Sonett, (1980b), Saturn's magnetosphere and its interaction with the solar wind, *J. Geophys. Res.*, *85*, 5655.

Southward, D. J. and M. G. Kivelson, (1987), Magnetospheric interchange instability, *J. Geophys. Res.*, **92**, 109-116.

Vasyliunas, V. M., Concepts of magnetospheric convection, In *The Magnetospheres of the Earth and Jupiter*, ed. V. Formisano, D. Reidel, Dordrecht, 179-188, 1975.

Wolfe, J. H., J. D. Mihalov, H. R. Collard, D. D. McKibbin, L. A. Frank and D. S. Intriligator, (1980), Preliminary results on the Plasma environment of Saturn from the Pioneer 11 plasma analyzer experiment, *Science*, *207*, 403.

FIGURE CAPTIONS

Figure 1. Plot of the cylindrical azimuthal, radial and vertical components of the flow within Saturn's magnetosphere as determined by *Richardson [1986]*, using Voyager 1 plasma data. The vertical blue lines indicate the L shell for the moons Tethys (4.95), Dione (6.3) and Rhea (8.85). For V_ϕ the diagonal red dashed line indicates corotation. The horizontal red lines for V_R and V_Z are at zero km/s.

Figure 2. Same as Figure 1, except now Voyager 2 plasma data is used.

Figure 3. Scatter plot of cylindrical radial velocity V_R versus angular velocity $\Omega = V_\phi/V_{COR}$ of the flow for Voyager 1 and Voyager 2.

Figure 4. Colorized rendition of the centrifugal interchange model of Saturn's aurora as proposed here. When the magnetosphere is compressed, the turbulence is enhanced along the dawn flank of the magnetosphere. Detached plasma islands break off from the plasma sheet outer boundary and move radially outward as the azimuthal flow increases in magnitude. The field aligned and radial current systems and their respond to compressions/expansions of the magnetosphere are shown. Individual flux tubes are shown as they are transported from mid-night to dawn to noon; they are color coded with red being hot plasma and blue cool plasma. They are hot after being emptied via plasmoid ejection down the tail and become cooler as the denser plasma builds up in the flux tubes (i.e., mixing of cold plasma with hot plasma). Plasmoid ejection near mid-night is illustrated, as well as lobe field lines in the tail. The flux tube boundaries are

corrugated to show presence of surface waves. The flux tubes are cut to show their 3D structure. The Kelvin-Helmholtz instability boundary along dawn flank is indicated. The figure shows an overall sense of rotation.

Figure 5. Plot of electron energy flux versus co-latitude of field lines mapped to Saturn's ionosphere. The top two panels show the data projected into the N and S hemispheres, the bottom plot shows the data plotted versus magnetic flux function evaluated for the *Connerney et al.* [1981, 1982] model (as used in the transformation). The ionospheric mapping employs a spheroidal ionosphere and the full SPV magnetic model. A rough conversion is 1 mW/m^2 ~ $2.5x10^{11}$ W of input power ~ 10 kR of UV aurora, but detailed energy-dependent efficiencies by *Gèrard et al.* [2004] need to be used to get a more accurate estimate. The black crosses are Voyager 1 data for $E < 200$ keV and the blue crosses are Voyager 2 data for 200 keV $< E <$ 1 MeV.

Figure 6. Field line mapping from Saturn's ionosphere, co-latitude θ, to the equatorial plane, equatorial radius ρ_e, for both the northern (solid line) and southern hemisphere (dashed line) of Saturn. The internal magnetic field and ring current by *Connerney et al.* [1981, 1982] were used.

Acknowledgements This work was supported by the Cassini Plasma Spectrometer (CAPS) Project and the CAPS team at Goddard Space Flight Center with support from L-3 Communications. JDR was supported by NASA planetary atmospheres grant NNG05GB27G and NASA contract 959203. We would also like to acknowledge the support by S.W.H. Cowley and E. Bunce from the University of Leicester in

the UK, who provided many illuminating scientific discussions on Saturn's aurora and assisted in the making of Figures 5 and 6 in our paper.

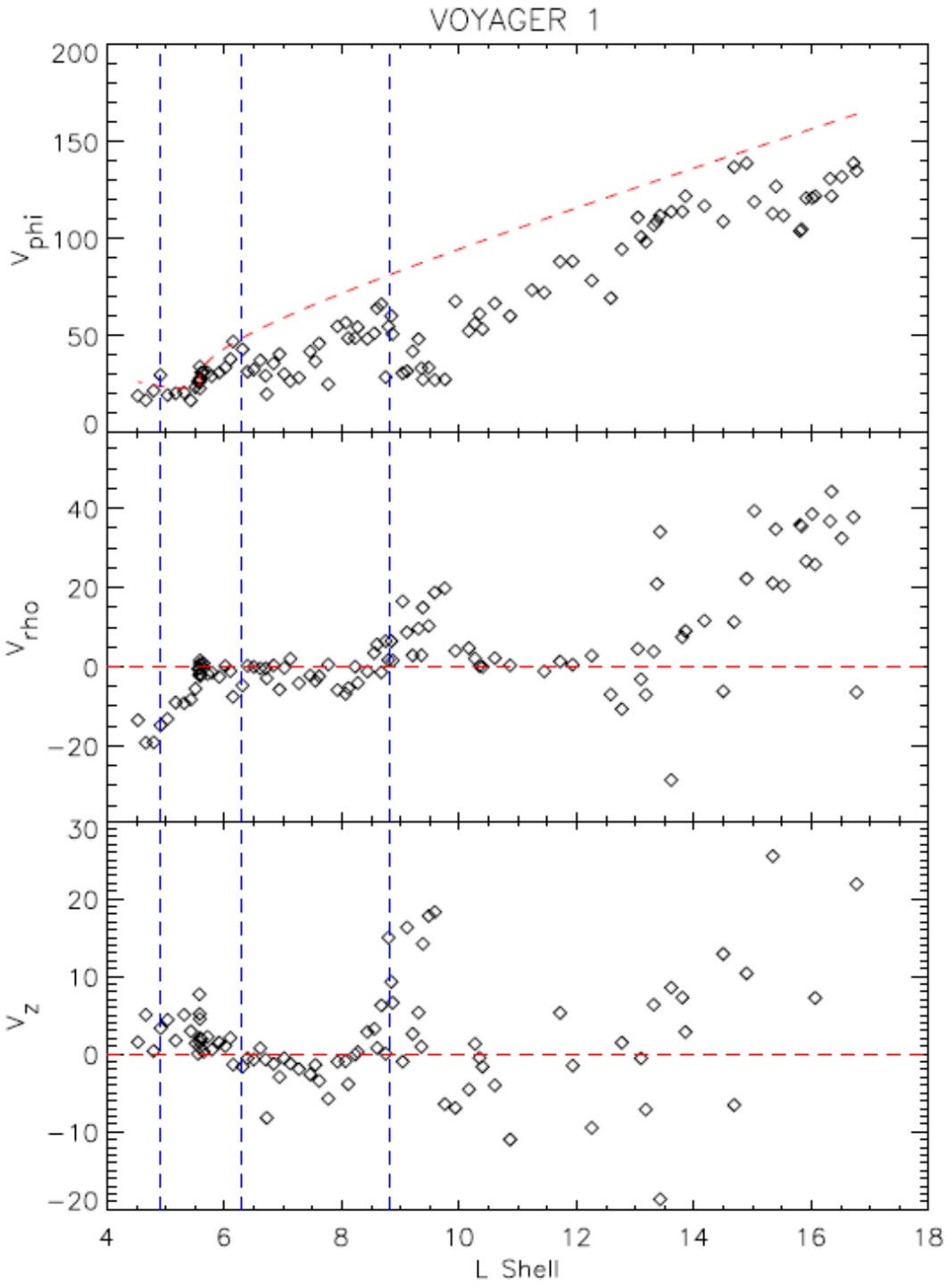
VOYAGER 1
V_phi
V_rho
V_z
L Shell
200
150
100
50
0
40
20
0
−20
30
20
10
0
−10
−20
4
6
8
10
12
14
16
18

Figure 1

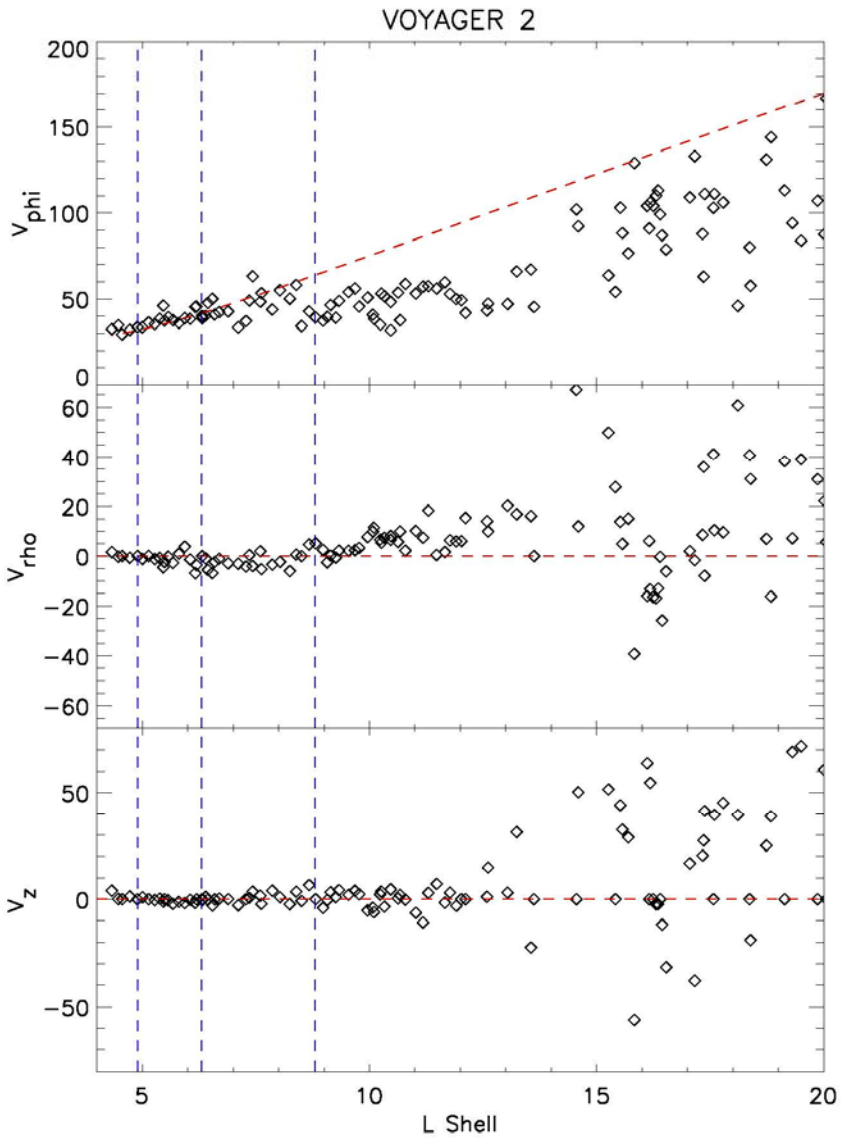
VOYAGER 2
200
150
100
50
0
V_{phi}
60
40
20
0
−20
−40
−60
V_{rho}
50
0
−50
V_z
5
10
15
20
L Shell

Figure 2

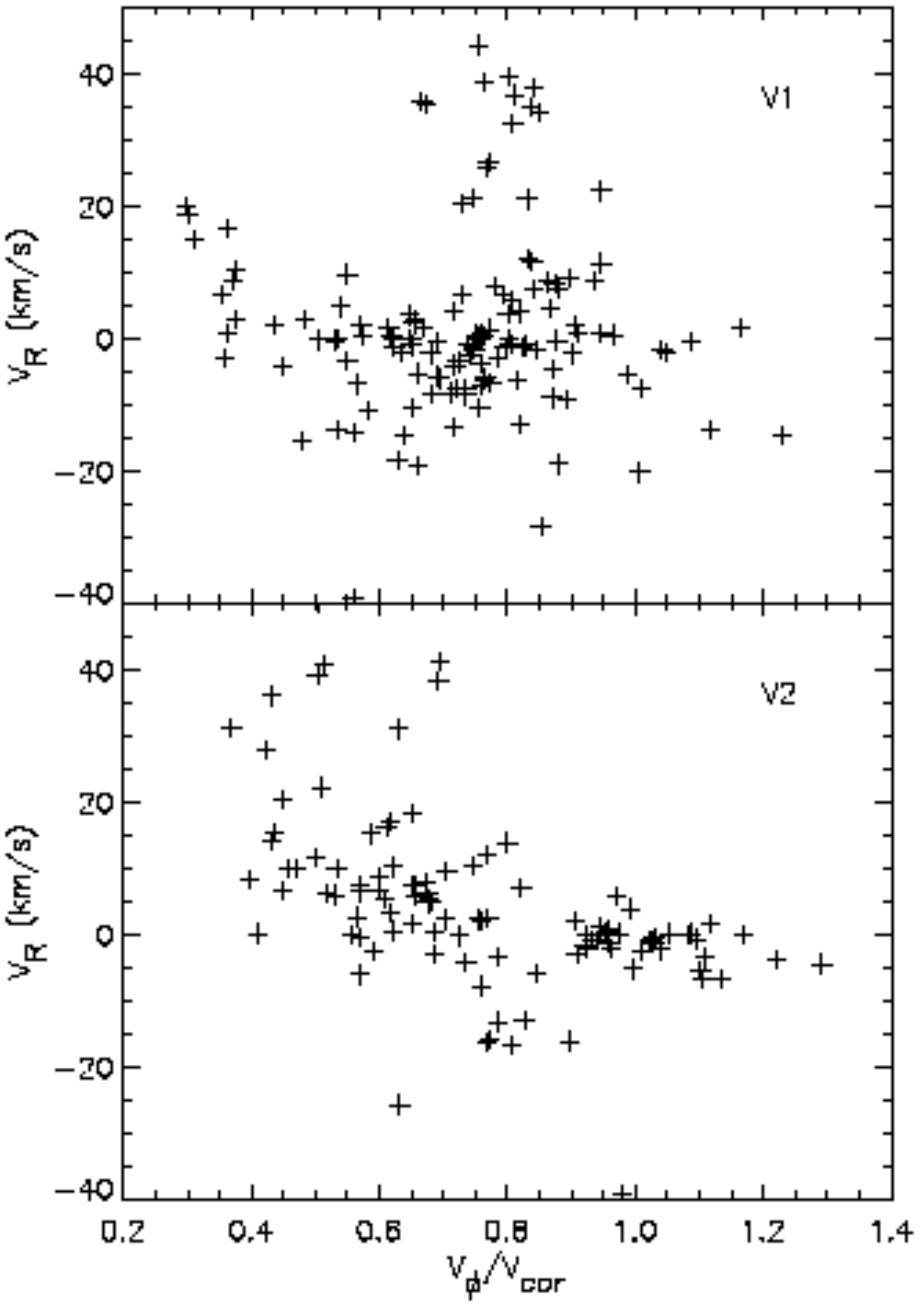

Figure 3

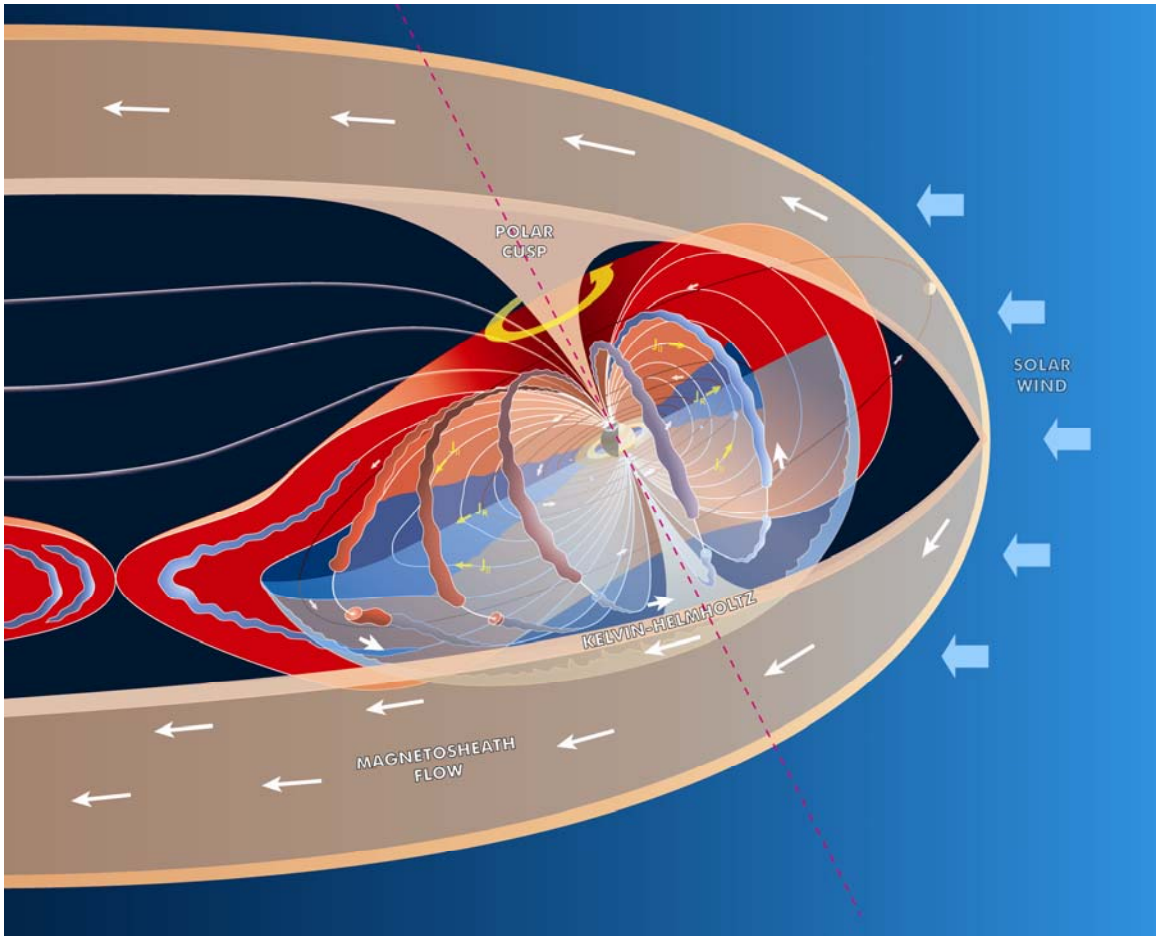
POLAR
CUSP
SOLAR
WIND
KELVIN-HELMHOLTZ
MAGNETOSHEATH
FLOW

Figure 4.

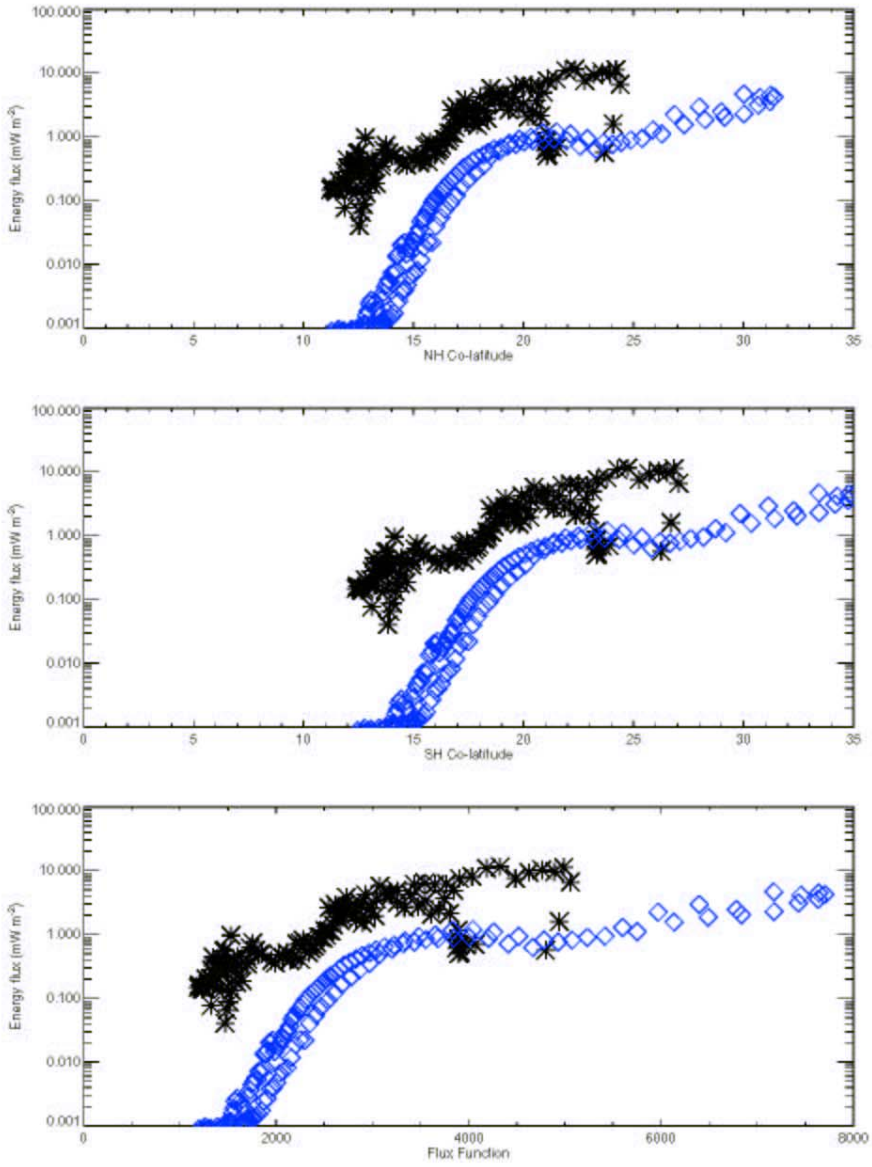
100.000
10.000
1.000
0.100
0.010
0.001
Energy flux (mW m-2)
0
5
10
15
20
25
30
35
NH Co-latitude
SH Co-latitude
2000
4000
6000
8000
Flux Function

Figure 5.

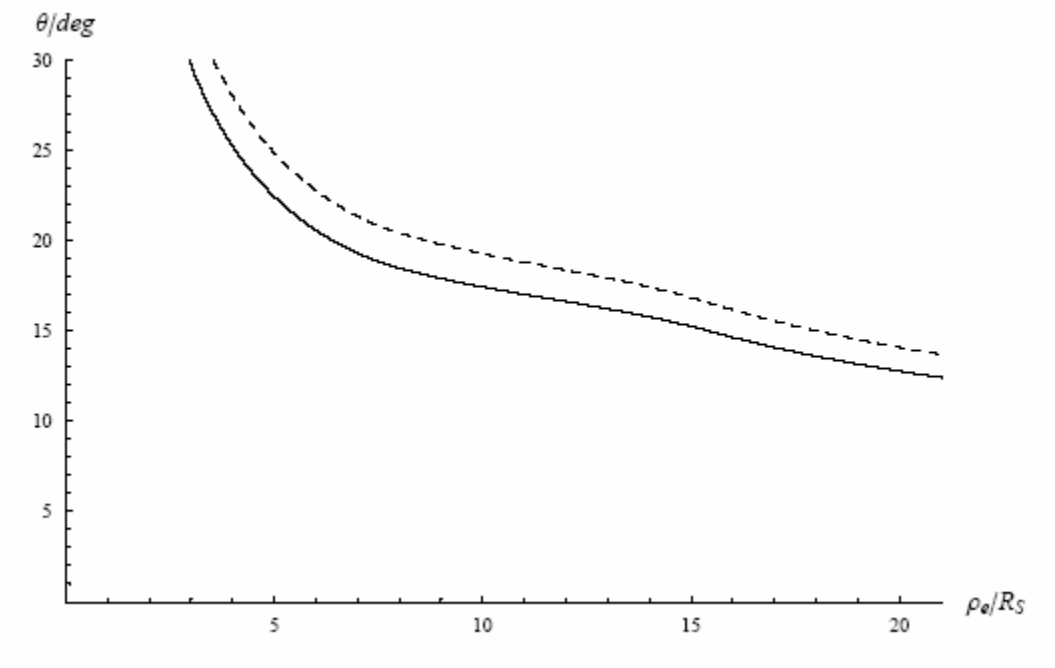

Figure 6.